UNIVERSITY OF WATERLOO

Design of an Improved Electromagnetic Projectile Device

Or: Coilgun 2: Electric Boogaloo

A report prepared for:
University of Waterloo

Prepared by:
Charles Holtforster

September 20th, 2020

Table of Contents

List of Figures

List of Tables

List of Equations

Summary

A thirteen-stage electromagnetic reluctance projectile device is designed for the dual purposes of producing a video that illuminates the design and production processes, as well as the completed device, and posing a personal challenge to the designer.

This type of device is commonly referred to as a “coilgun” because of its use of solenoids wound about the barrel and is not to be confused with a railgun. Due to fears of adverse effects on video distribution on YouTube, the name “gauss cannon” was used in official documentation and working video titles. Powered by a 12-cell lithium ion battery pack, the device will propel more than ten 9-gram steel projectiles per second at approximately 100m/s, each carrying 50J of energy. The gun satisfies Canadian criteria for not being a firearm.

A visually interesting mechanical design for the gun is produced that does not compromise operator safety while still allowing operability and maintainability. The design accommodates operation of the device as a shoulder-fired weapon.

Parallel-connected Metal-oxide-semiconductor-field-effect-transistors (MOSFETs) are used for control of the electromagnetic elements. A method for achieving optimal performance is determined. Printed circuit boards (PCBs) are designed for the control systems and power systems. A safety system was implemented to prevent unintended firing. A method for determining optimal timing parameters was developed and utilized to maximize muzzle velocity.

This updated design seeks to achieve the gains in projectile velocity, weight reduction, and increased rate of fire discussed in the report on the 2019 design. Though the design is complete, the gun remains in the prototyping phase. Completion is expected in 2021.

1 Introduction

The development of this device began as a personal endeavour, separate from the goals of Hacksmith Entertainment. In late July 2020, it was decided that the production of the coilgun would continue with funding and backing from Hacksmith.

The primary business purpose of this undertaking is to make a video to be posted on the Hacksmith Entertainment YouTube channel. Due to rising concerns over the advertising impact of a video about guns on YouTube, the project may become once again a personal endeavour for the sake of learning and skill development.

A coilgun propels a projectile by means of one or more high strength hollow core solenoids that exert a force on the projectile, moving the projectile towards the center of the solenoid. The solenoid's magnetic field is switched off when the projectile approaches the solenoid's center, permitting the projectile to continue forward under its own momentum. Several of these solenoids, referred to as stages, are placed in linear succession such that earlier stages direct the projectile into later stages, resulting in acceleration of the projectile.

1.1 Objective

The intended outcome of this project is to produce a device that, by means of magnetic reluctance, projects many steel slugs in rapid succession to achieve acts of gratuitous destruction outstripping those achieved by the Hacksmith Coilgun, model of 2019 (HSCG19).

1.2 Constraints and Criteria

1.2.1 Constraints

As with the HSCG19, the device was required to:

- Not be a firearm under Canadian law. This is achieved by either
    - not exceeding a muzzle velocity of 152.4 m/s, or
    - not exceeding a muzzle energy of 5.7J [1]
- Look cool on video (i.e.: visually and audibly interesting).
- Not pose a safety risk to the operator.
- Achieve electrical isolation between user controls and any high-voltage circuitry.

- Have all electrical inputs fuse protected to prevent battery fires.
- Not exceed the maximum safe burst discharge current rating of the battery system.
- Have a weight low enough that a single person can pick up, hold, and point the assembled device.
- Be operable in a rifle-like manner.
- Be maintainable, and permit replacement of all electrical components after non-destructive disassembly.

In addition to the original requirements, it was also required that the device:

- Be capable of repeated fire from a magazine without manual user intervention.
- Be capable of sustained fully automatic firing, that is, multiple projectiles for a single user action.

1.2.2 Criteria

- Cost should be minimized.
- Ease of assembly should prevail over cost or weight reductions, as all assembly work is done manually.
- All other things being equal, a higher muzzle velocity is preferred, provided it does not exceed the 152.4 m/s legal limit.
- All other things being equal, a higher rate of fire is preferred.

2 Design Considerations

2.1 Ammunition

Several key characteristics must be determined before proceeding with detailed design. The size of ammunition in use drives practically every other aspect of the entire gun, from mechanical to electrical design. It may then come as a surprise that their selection was almost entirely arbitrary.

The ammunition selected were 6mm diameter alloy steel dowel pins, 40mm long. These projectiles were chosen for having already been purchased for a previous coilgun design, where they had been selected for no serious reason except their subjectively bullet-like shape. The selection was made from the sizes of steel dowel pin available from McMaster-Carr.

This new size of projectile is dramatically smaller than that of HSCG19, as shown in Figure 1. The reduced size and mass means that more stages, or higher power stages, will be required to produce similar kinetic energy to the older design, although higher speeds are achieved per unit energy. While the energy reduction (all other things being equal) runs in contradiction to the goal of increasing destruction, the reduced size dramatically increases the manageability of the projectile for purposes of magazine feeding.

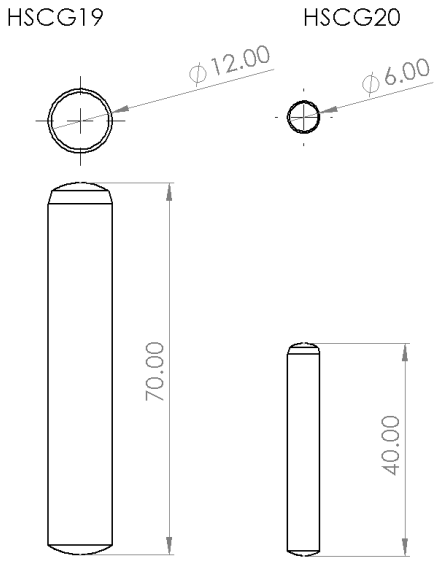

Figure 1 Projectile size comparison, HSCG19 and HSCG20

2.2 Thermodynamic limits

Given the understanding the gun would be fully automatic and powered by a lithium polymer battery, as well as the assumption that the efficiency would be comparable to the previous design, some estimates were made of the achievable performance. Lithium polymer batteries were sourced which, for a price deemed reasonable prior to the project becoming associated with Hacksmith, could produce 1540A at 50V, or 77kW. The selected model was the Turnigy *Rapid* 5500mAh 4S2P 140C battery pack [2]. For a modest rate of fire of 10 Hz and an optimistic system efficiency of 5%, this maximum power yields a maximum projectile energy given by

$$u_p \leq \eta P \frac{1}{f} = 5\% * 77000W * 1/(10Hz) = 385J$$

For a more optimistic rate of fire of 40Hz, this produced a maximum projectile energy of 96J. Since the projectile cannot have work done to it except when it is within the gun, the maximum energy is also a factor of the projectile velocity, and subsequently mass – for the same energy, a larger projectile will move more slowly and so will be in the barrel longer, permitting a larger total impulse to be applied. It is not expected that the projectile will achieve the maximum possible energy.

Storing all the available energy to consume it within the firing window – that being the time when the projectile is within the accelerator – is difficult. At 10Hz, the available energy is 7.7kJ. Storing 7.7kJ in a capacitor, even at high voltages, requires very large capacitors. At the system voltage of 50V, 6.2 farad of capacitance would be required, which would make achieving the portability requirement impossible.

2.3 Thermal considerations

The other key limiting factor is the poor efficiency of coilguns. 5% efficiency is reasonable to expect. If 5% of 77kW is getting into the projectile, the remaining 73kW will be consumed somewhere else. This will result in the production of heat throughout electrical and mechanical resistance. This power is dissipated primarily in the resistance of the batteries, the resistance of the solenoids, and the junction potential of the flyback diode. The MOSFETs also heat up due to their internal resistance, as do the busbars, PCBs, and power wires.

Since, regardless of the exact details, the system will use a large fraction of the available 1540A, the matter of heat must be addressed. The gun uniformly heating up at any appreciable fraction of 73kW would likely violate several constraints, including the operability requirement when the device becomes too hot to hold, and the reliability requirement when some component fails due to overheating, and, as witnessed in HSCG19, cause a cascading failure that ends in the destruction of multiple stages. A key engineered control in avoiding the melting of the gun is limiting the size and quantity of the magazines produced such that firing enough ammunition in a short period of time to damage the gun requires concerted effort.

3 Electrical Development

The development of a coilgun had been previously studied at *Hacksmith* in 2019, resulting in the Hacksmith Coilgun model of 2019, regrettably named *Boaty McGunface*. This previous version achieved modest power and only single-shot operation. As described in the report on the design of the earlier model, a coilgun in its simplest form consists of a hollow solenoid, a timer, a switch, a power supply, and a projectile [3]. The solenoid's magnetic field is switched on when the projectile is behind the solenoid, producing a force on the projectile, and instantaneously turned off when the projectile arrives at the centre point of the solenoid.

The electrical system is required to switch the coil, reduce the coil current without sustaining damage, and time these actions optimally. These electronics must be supplied with power to permit their operation. The coils should be designed to make optimal use of all available power. In an automatic coilgun, several other tasks must be managed. To achieve repeating fire, an electromechanical subsystem must be implemented to introduce rounds into the barrel at the appropriate time and verify their presence. A magazine must also be developed to permit repeating fire, though that is not a matter of electrical design. The correct feeding of rounds from the magazine must be verified and controlled.

3.1 Power supply selection

For fully automatic operation, the only appropriate power supply for a portable coilgun is a high-current lithium-ion battery.

The selected batteries are rated at $280hr^{-1}$, also known as 280C [2], discharge rate for a ten second burst, with a capacity of 5.5Ahr. This gives a total available current of 1540A for a ten second

window. With the assumption that it would be unreasonable to produce a system that could sustain that much current draw for ten seconds, these batteries, manufactured by Turnigy, were selected. Three 4-cell assemblies were purchased, providing a peak voltage of 50V. The total available instantaneous power is 77,000W.

3.2 Performance simulation

The key difference in the development of the HSCG20 as compared to the HSCG19 was the emphasis placed on determining behaviour characteristics in advance of production of a prototype. The freely available magnetics simulation software Finite Element Method Magnetics (FEMM) was used to determine expected system performance. A computer program provided in the appendix was written in Python to perform an axisymmetric magnetostatics simulation, Figure 2, in FEMM of the accelerator coil and projectile at finite distance steps of the projectile towards and through the coil. The force applied to the projectile at each step could then be integrated to find the total work done, and so the energy imparted to the projectile. In conjunction with the characteristics of the available batteries and some estimates for the resistance of the rest of the electrical delivery system, strong predictions could be made as to the energy imparted per stage under ideal circumstances.

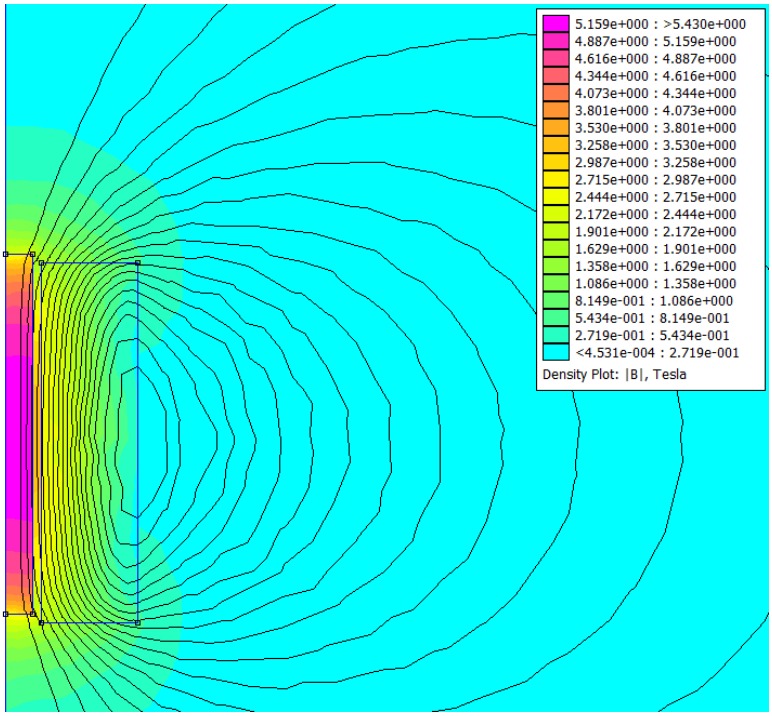

Figure 2 Single timestep of simulation in FEMM. Bore axis along left edge of image. Flux density by colour.

Comparing the resultant work of various coil designs revealed that, for a given power supply system, maximum work is achieved when the coil resistance matches that of the power supply system. While this result is obvious in hindsight, it was fundamental in guiding future design effort. Though this produces the highest performance for a single stage in isolation, the current in the coils – those being inductors – cannot change instantaneously, and so several coils must be activated at once to produce the desired forces at a later point in time. Since multiple loads will be active at once, their parallel resistance, rather than their individual resistance, could be impedance matched to the supply resistance. This, however, tends to maximize stress on the power electronics. The results of the simulation are provided in Figure 3.

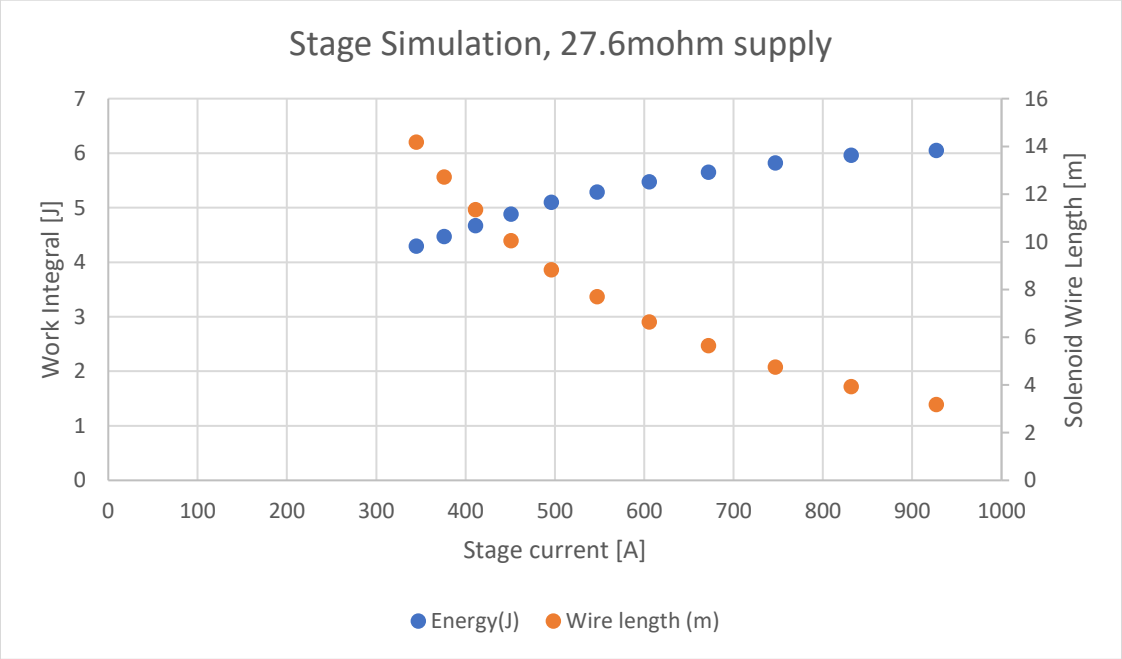

Figure 3 Per-stage projectile work vs. current consumption for several wire lengths.

The simulation shows a clear relation between coil current and stage energy. Trading off some stage energy for a reduction in coil current and MOSFET heating was deemed worthwhile, so an operating point 20% below the peak stage performance was selected, nominally drawing 549A and delivering 4.7J per stage, permitting the simultaneous activation of two stages at steady state. This stage design corresponds to 7500 mm of 14AWG magnet wire being wound into each coil.

3.3 Stage count

In the ideal case, the projectile kinetic energy, or muzzle energy, of a coilgun is linearly proportional to the number of stages on the device, as per Equation 1 Projectile energy and stage count relation. Since the simulation produces an estimate of the kinetic energy produced per stage, the maximum number of stages legally permitted can be found by taking the velocity for a given kinetic energy and solving for the legal limit of 152.4m/s.

Equation 1 Projectile energy and stage count relation

$$E_k = \frac{1}{2}mv^2 = nE_{ks}$$

$$n = \frac{\frac{1}{2}mv^2}{E_{ks}}$$

Since the stage count scales with the square of velocity, it is impractical to achieve the legal limit with a 9-gram projectile if each stage adds 4.5J, as the resulting accelerator assembly would have 24 stages, making it 1300mm long. With the addition of a magazine well and loader assembly, the completed gun would be rather large, at ~1400mm, roughly equivalent to the length of the Barret M82A1 anti-materiel rifle [4], which is usually not considered a readily shoulder-fired weapon. The arbitrary decision of 10 stages was made initially, then superseded with 13 stages when a mechanical design with a fixed maximum length was selected and use of every available millimetre of length was determined to be in the best of interests of performance.

3.4 Power electronics

3.4.1 Stage switch board

In light of the costs incurred by HSCG19 due to stage switch failure destroying the entire stage PCB, and the increased per-stage cost due to the computerized stage controller in HSCG20, the decision was made to split the stage control and feedback from the power switch elements, the latter being dramatically more likely to fail irreparably. The power switch board assembly is shown in Figure 4. Failed low power components can usually be replaced on the PCB, while high power components often destroy the PCB with them in the process, as in Figure 5.

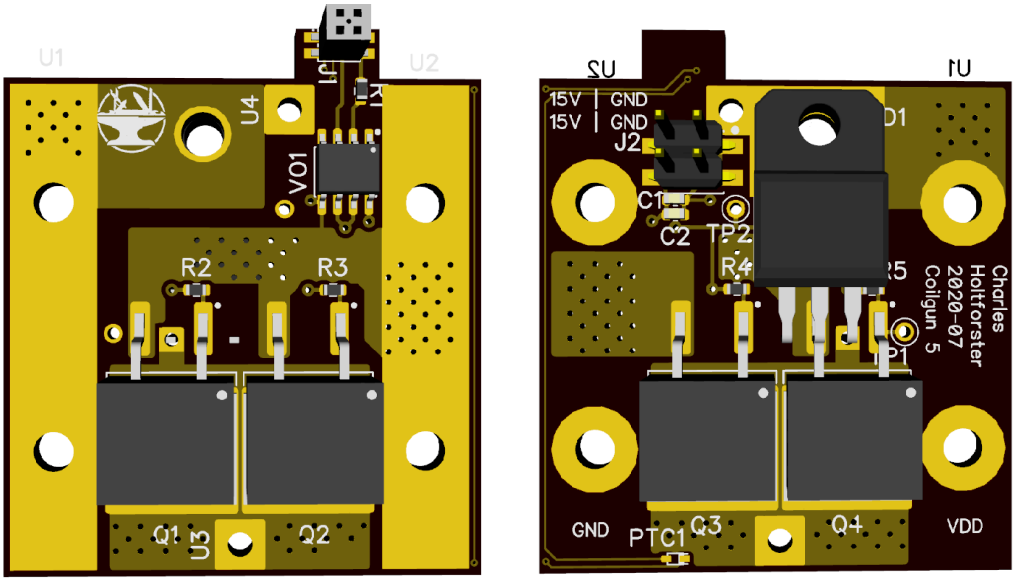

Figure 4 Assembled stage switch board. Top (left) and bottom (right). D1 is non-representative of installed component

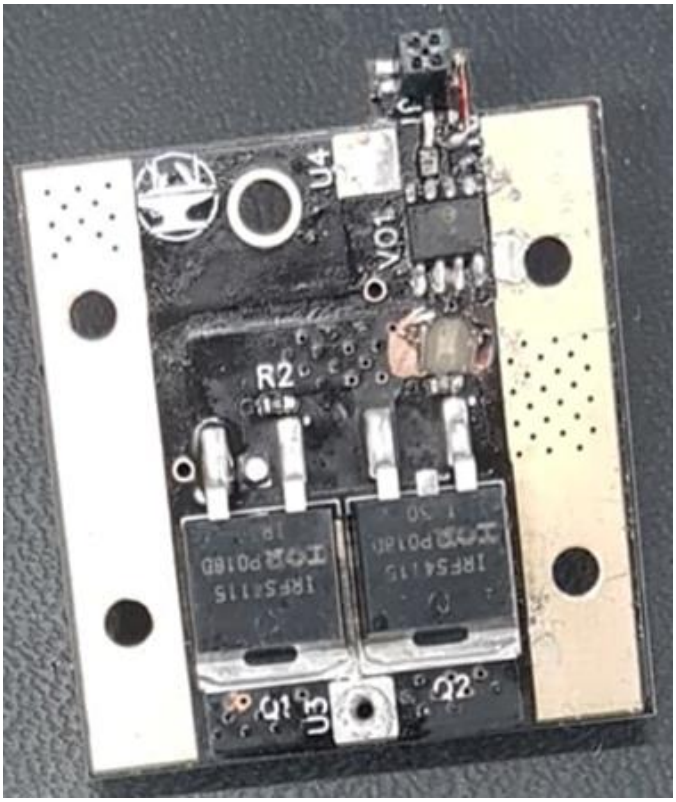

Figure 5 A failed power switch board. Note the crater between Q2 and VO1 due to the circuit failing closed.

3.4.2 High current switch

The use of a Metal-Oxide Semiconductor Field Effect Transistor (MOSFET) was determined to be the optimal switching solution in HSCG19 [5]. This decision will not be examined any further.

To increase the maximum current switchable in a stage, paralleled MOSFETs are used. Paralleling MOSFETs is typically used to decrease the heatsinking requirements, as the dissipation per device decreases with the square of the device count given matched devices. In this case, however, the paralleled MOSFETs are required solely to permit more current to be controlled, as the expected coil current vastly outstrips the capabilities of any board-mount transistor on the market.

The IRFS4115TRLPBF N-channel power MOSFET, introduced by International Rectifier in 2008 and used previously in the HSCG19, is nominally capable of conducting 195A continuously when appropriately heatsinked. A similar level of performance can be expected with a 10ms pulse, as shown in the Safe Operating Area curve, Figure 6, provided in the component datasheet [6].

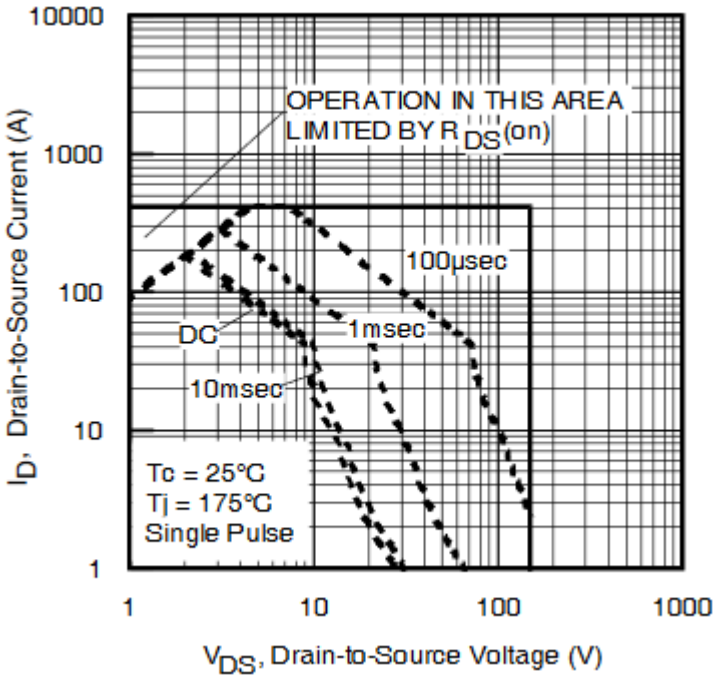

Figure 6 IRFS4115TRLPBF safe operating area curve, from Infineon [6]

The device is capable of switching 150V, which exceeds the required 50V by a wide margin. With the anticipated design requiring somewhere around 600A per stage, more than one IRFS4115TRLPBF would be required. NXP Semiconductors' Application Note 11599 on parallel power MOSFETs recommend a significant current capacity margin be added to accommodate the

possible differences in conduction resistance between paralleled devices, noting explicitly that "The power capability of a group of n MOSFETs never achieves n times the power capability of a single MOSFET" [7]. For this reason, a group of four MOSFETs is used, providing a 780A theoretical capacity, and a 180A margin of current capacity, or a 1.3 factor of safety.

3.4.3 Flyback suppression

The inductive nature of a solenoid requires that a flyback suppression be included in the power switch circuit. Without flyback suppression, the voltage at the switched side of the inductive load will rise as the energy stored in the inductor's magnetic field converts itself to capacitively stored energy between the high and low side of the switch. For a typical MOSFET drain capacitance of approximately 1nF, this would be accomplished at around 300kV. Before this can happen, the MOSFETs will enter avalanche mode and very likely be destroyed. Flyback suppression refers to a circuit element responsible for permitting the flow of current in the load after the switch has turned off to prevent failure of the switch. This is most readily accomplished with a diode placed antiparallel to the inductor. Other methods of flyback suppression are possible and even preferable under certain circumstances [8].

For the purposes of the coilgun, a high-power diode was chosen. Performance gains stand to be made by introducing larger potential in series with the return current path, assuming the increased potential does not exceed the maximum drain voltage on the power MOSFET array. While this could be accomplished by installing several diodes in series, the dramatically increased cost does not produce a significant change, since most of the voltage drop will be due to the resistance of the inductor itself rather than the forward voltage of even a large number of diodes.

The nature of this current decay can be modelled as a differential equation, written in Equation 2. Since the diode forward voltage component is essentially negligible, the decay can be predicted to follow the standard resistor-inductor (RL) decay form.

Equation 2 Flyback current decay differential equation

$$\frac{di}{dt} = \frac{V_{fd}(i) + R_{coil}i + R_{circuit}i}{L}$$

$$V_{fd}(i) \approx 0$$

$$i(t) = i_{initial}e^{-\frac{t}{L/(R_{coil}+R_{circuit})}}$$

Increasing the rate of decay in the circuit by maximizing the resistance will clearly result in faster current reduction. An ideal appropriate resistor would be inexpensive, compact, and capable of handling an essentially instantaneous pulse of dissipated thermal energy inside of it on the order of tens of joules. The ideal resistance value would see the forward voltage on the switch barely reach the breakdown voltage of the MOSFET - in the case of the IRFS4115TRLPBF, 150V. This resistance can be found, shown in Equation 2.

Equation 3 Flyback resistor value calculation

$$V_{DSS(MAX)} \geq V_{supply} + Ri_{initial}$$

$$R \leq \frac{V_{DSS(MAX)} - V_{supply}}{i_{initial}} = \frac{150V - 50V}{600A} = 0.167\Omega$$

Unfortunately, a part matching this description could not be found, and likely does not exist. The energy dissipated in the flyback circuit is equal to the stored energy in the inductor, which, for an estimated 600A and 247μH is equal to 44.5J. Since the coil resistance is comparatively low, at 66mΩ, the flyback resistor would absorb much of this energy, approximately around 35J, in approximately two milliseconds, producing 17500W of thermal power. The largest surface-mount resistors from Ohmite, the TDH50 series, are rated for 50W of continuous dissipation with proper heatsinking [9], and even that cannot be provided due to space constraints. Larger formats of resistor are available but would dramatically complicate the assembly of the gun and interfere with the critical appearance constraint.

In the end, the increased design difficulty due to failure, the increased production cost, the increased risk of redesign while on a tight timeline, and the dramatically increased risk of the assembly explosively jettisoning resistor shrapnel during testing made the use of the flyback resistor unfavourable.

The STMicroelectronics FERD40H100S [10] is used as the primary flyback diode, being able to handle the large currents involved and operate at reverse voltages of 100V, far in excess of the 50V of the batteries in the gun. For size constraint reasons, the device was soldered by the flange to an exposed pad on the PCB, while the cathode leg was removed from the package and the remaining two anode legs bridged to pass through a single through hole in the board.

3.4.4 Switch driving

To control a MOSFET at high speeds and high powers, a gate voltage exceeding typical microcontroller operating voltages is required. 15V is a typical gate voltage. A gate driver circuit is used to permit control of the MOSFET by the microcontroller. This circuit is available as a single component for ease of assembly.

For HSCG19, ON Semiconductor's FOD3182 gate driver integrated circuit (IC) was used [5]. This was replaced with the Silicon Labs SI8261BBC-C-ISR [11], which is functionally similar to the FOD3182 but available in a more compact package.

This device is driven by current control on the input side. The driver side connects the output to the ground supply rail unless a certain current is passed through the input side, in which case it connects the output to the positive voltage supply rail. This permits easy driving of the MOSFET's gate at a higher voltage greater than the operating voltage of the control circuitry.

Still available in gross excess from previous coilgun work, a 15V TDK-Lambda PAH50S48-15/V power supply is used. A printed circuit board was produced to house the 15V and 5V supplies, as well as the ancillary hardware [12] required.

3.4.5 MOSFET Thermals

The heating of the MOSFETs is the most likely source of failure in the gun. Passing several hundred amps through each transistor produces a large spike of heat within the transistor junction with each shot. The MOSFET will fail if the junction temperature exceeds the manufacturer's specified $T_{J(max)}$ value. In the case of the IRFS4115TRLPBF this value is 175°C. The heat transfer from the junction to ambient air can be modelled with time-domain electronics modelling tools, including Linear Technologies' LTSpice.

Heat generation in the MOSFET is the same as in a similarly valued resistor. The maximum drain-to-source resistance for this MOSFET is 12.1mΩ. Under the pessimistic assumption that current sharing between the devices is poor, the maximum expected current is taken as the maximum transistor current – 195A. The resistive heat generated under these conditions is 464 watts.

Estimates for the junction and die thermal properties can be taken directly from the component datasheet, while estimates for the case thermal properties can be made from first principles. The

thermal circuit diagram with LTSpice source syntax is shown in Figure 7. *Tj* represents the junction temperature, Td the die temperature, Tc the case temperature, and Ta the ambient temperature.

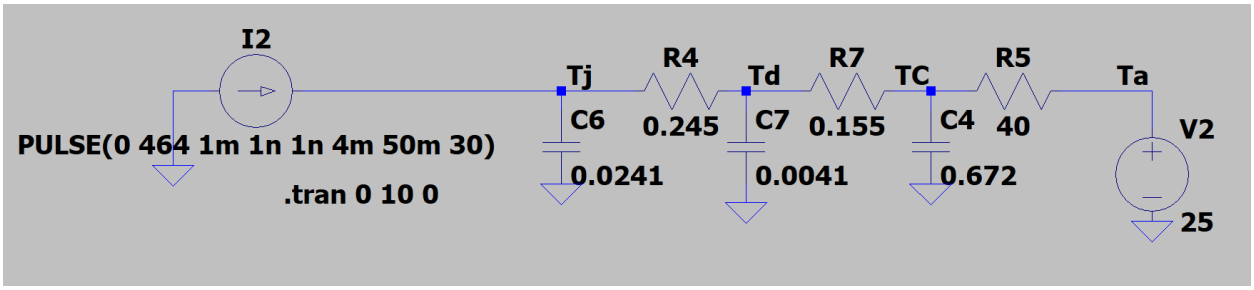

Figure 7 Thermal simulation circuit

The simulation parameters can be adjusted. As depicted, heat is produced every 50ms for 4ms, for a total of 1.5s, or 30 pulses. This represents the first stage firing, on automatic, at 20Hz for an entire magazine. This simulation makes several simplifications regarding the heat pulse train, fully ignoring both the heat produced at turn-on and turn-off of the MOSFET, as well as the absence of heat produced during the current rise. The results, Figure 8, show the junction temperature in green. Under the simulated conditions, the 175°C temperature limit is not exceeded in firing a 30-round magazine.

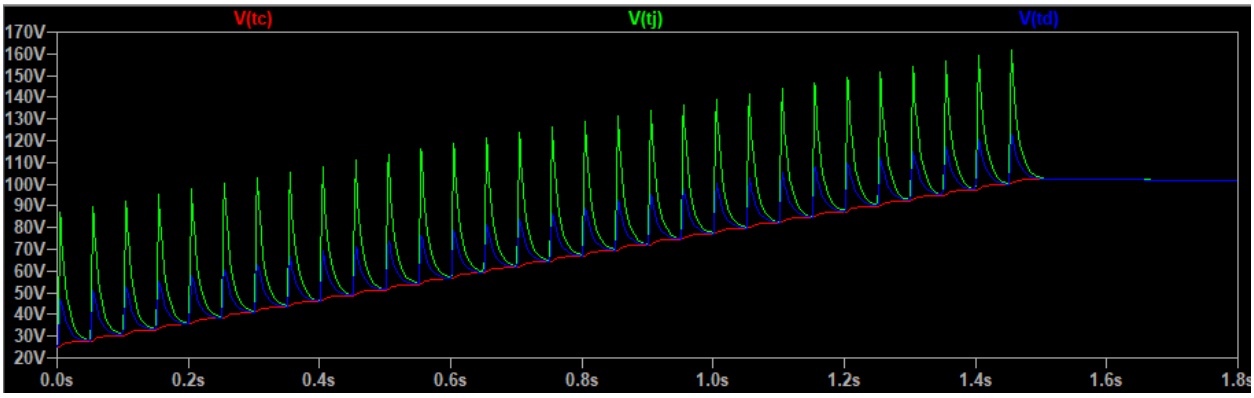

Figure 8 Thermal simulation results for 464W, 4ms firing time, 50ms firing interval, and 30 repetitions. Maximum temperature 162°C. Note that the vertical axis, marked in volts, represents °C.

The slow decay of the case temperature would have the MOSFETs overheat shortly if more ammunition were fired, however. This limit occurs after approximately 35 rounds. Through this simulation, the efficacy of heatsinks can be tested (Figure 9). An excellent heatsink with a thermal conductivity to ambient of 5K/W and representative thermal mass of 0.5J/K is tested by adding another node to the thermal circuit.

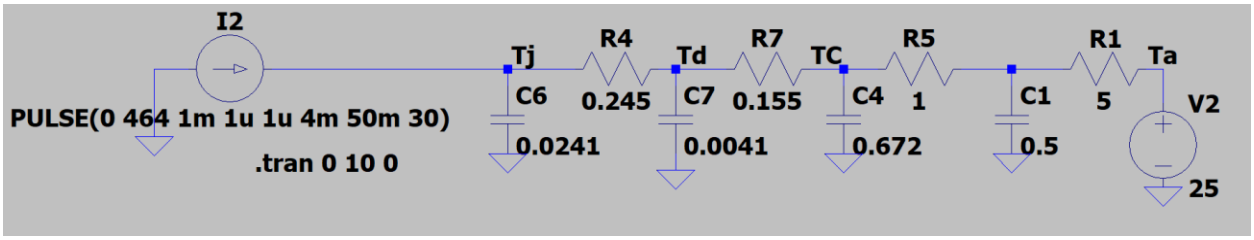

Figure 9 Thermal simulation circuit with representative excellent heatsink.

The results of the simulation, Figure 10, show a reduction in peak junction temperature to 135°C. However, a 5°C/W heatsink cannot be fit inside of the gun, especially not on every MOSFET in every stage, and certainly not without dramatically increasing costs.

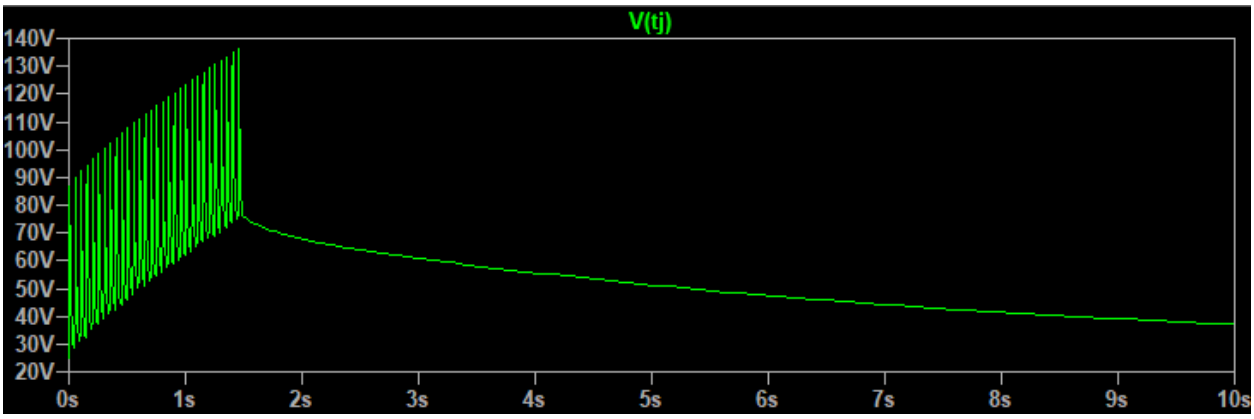

Figure 10 Thermal simulation results with excellent heatsink

A more practical option is the introduction of thermal ballast. A cheap heatsink can be used to introduce additional thermal mass to heat up before the MOSFETs fail, ultimately permitting the firing of more rounds without cooling the gun down. Because of this effect, the use of a dedicated heatsink is superfluous; attaching a block of copper to the tops of the MOSFETs will serve just as well. A simulation, Figure 11, with the original 40K/W impedance to ambient but with a much larger 1.4J/K thermal mass in the heatsink shows improvement, Figure 12, compared to the excellent heatsink, with a peak temperature of 130°C.

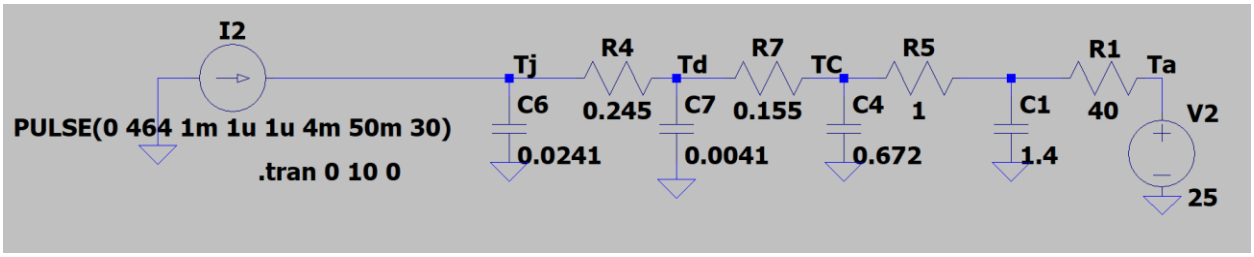

Figure 11 Thermal simulation circuit with unaided thermal transfer and large thermal mass

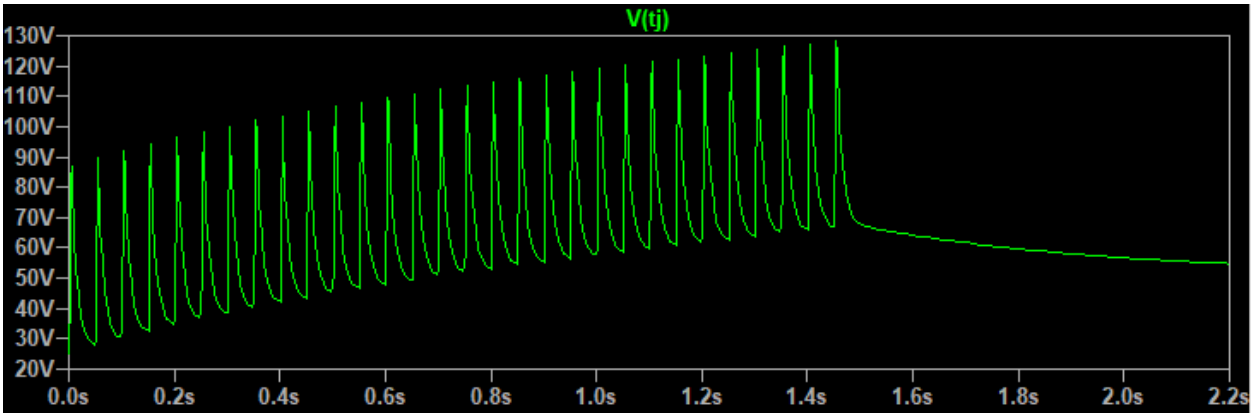

Figure 12 Thermal simulation results with unaided thermal transfer and large thermal mass

Given the simplicity, ease, low cost, and effectiveness of increasing the transistor thermal mass, this option is the clear correct path forward for increasing system reliability. The 1.4J/K figure represents approximately the maximum size of copper plate that could be attached to each MOSFET without impacting the gun's aesthetics. Proceeding under the assumption that this is as good as solid-state thermal absorption can get, the maximum sustained rate of fire and maximum burst length, i.e., magazine size, can be found experimentally in the simulation. A 20-round burst at 20Hz every 30s with an ambient temperature of 25°C is indefinitely sustainable. Alternately, two 20-round bursts at 20Hz with a 10s reload delay will immediately approach the thermal limit, at 174°C after the 40th round. At a more realistic 10Hz, a 20-round burst every 25 seconds can be sustained indefinitely.

A mechanism for proactively detecting overheating conditions in the accelerator is certainly required. This will be achieved with a thermistor mounted to the power switch board near the MOSFETs, whose signal will be relayed to the main controller via the stage controller

3.5 Control electronics

3.5.1 System control bus

Several practical limitations to the control scheme used in HSCG19 exist. Running individual wires to each stage for both the fire control of photogate feedback signal produced a very large signal bus, requiring intricate custom cable assemblies to be made. The use of a common signal bus was deemed necessary to avoid this for the larger stage count in HSCG20. For simplicity and speed, a parallel bus was implemented. The main controller computer in the stock of the gun drives a bus with four address bits, two output data bits, one input data bit, and one analog data input.

These output data bits represented the *fire command* and *write enable* signals, while the input signals represented the photogate state for the selected stage and the temperature sensor reading of the selected stage.

For each stage, this design required some logic element to determine the correct state of the power switch and whether to enable transmission of feedback data. While a discrete logic solution would have been trivial, the use of a small microcontroller was cheaper and left more room for adjustment and repair in the event of design mistakes. Each stage controller board housed an ATMega44a microcontroller, a set of LEDs, a phototransistor signal buffer, and a switchable amplifier for the thermistor output. The program on the microcontroller would, upon seeing its address on the bus and the *write enable* signal, copy the state of the *fire command* signal onto its local fire output and set a *txen* (transmission enable) signal on the board. The transmission enable signal was passed to a tristate buffer to transmit the photogate signal onto the bus digital input data line, and to the switchable amplifier to transmit the thermistor state onto the bus analog data input line.

To ensure the effectiveness of the "safety" switch at the operator's controls, the 5V signal from that switch is used directly as the anode signal for the gate drivers. This signal is passed along the bus via a dedicated line. A reference ground for the thermistor amplifier is included in the bus to mitigate interference and noise due to current in the power ground signal. While this should provide a degree of immunity against run-of-the-mill ground noise, it is not expected to provide any useful protection against the induced voltage from the accelerator stages firing. Readback of the thermal sensors will not be attempted during firing.

3.5.2 Feedback

For eventually automatically tuning the device, some form of feedback for the projectile position is required. The use of an infrared light emitting diode (LED) and phototransistor permits the reliable detection of a passing projectile. This was tested with discrete through hole components and found to function reliably even with minor misalignment of the transmitting and receiving devices, a problem encountered on HSCG19. To further mitigate risks of optical element misalignment, the two devices were designed onto the stage controller PCB as fixed board-mount elements, preventing them from shifting positions except under catastrophic stress.

3.5.3 Stage controller board design

Each stage contains a power switch PCB and a controller PCB, Figure 13. The controller PCB nests into the forward separator of that stage, oriented normal to the bore axis of the gun. A 14-pin ribbon cable connection is provided for the shared data bus, permitting connection for each stage without interfering with the cable routing. The connection to the power switch PCB stems from the bottom of the board.

Status LEDs are provided on a tab on the left-hand-side of the board which extends to the edge of the accelerator assembly, permitting the user to quickly identify major errors with the accelerator. These four LEDs provide an indication of whether the stage is receiving 5V power (D1, green), whether the gun is armed (D3, amber), whether the stage is transmitting and receiving data (D2, blue), and whether the stage is currently firing (D4, red).

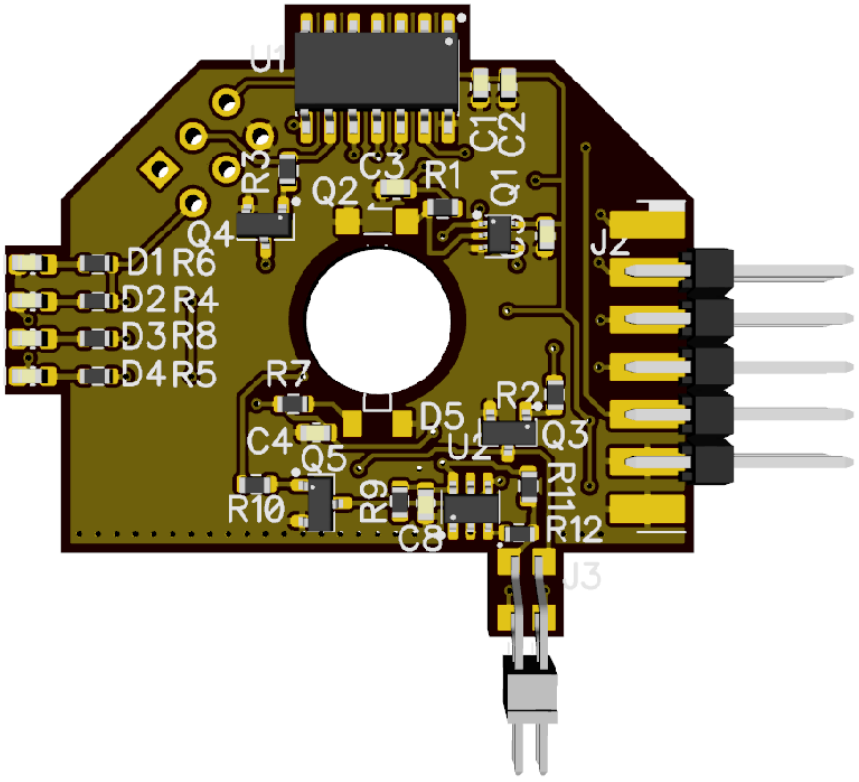

Figure 13 Rendering of stage controller PCB with nonrepresentative components. Note hole through board.

The PCB straddles the bore of the gun, that is, the projectile passes through a hole in the center of the PCB. This permits the photogate to be built directly onto the PCB. This also serves to increase the available surface area for the PCB. The programming header footprint is placed on the rear of

the board, though the through holes are visible from the front. This placement permits reprogramming of the board while it is installed in a stage assembly.

3.5.4 Main controller board

The operation of the gun is managed by the main controller board (Figure 14). This PCB receives user input and sensor feedback, and provides control output of the accelerator stages, injector solenoids, debugging LEDs, and the safety disconnect relay. The processing is managed by a Teensy 3.5 microcontroller development board. The control of the injector solenoids is managed via a set of low-side switching N-channel MOSFET with flyback diodes connected to isolating gate drivers. While only two injector solenoids are required by the design, future work may require other high-power outputs, so four outputs are provided.

The thermal sensing signal is buffered by an operational amplifier circuit. The digital output lines to the control bus are buffered by a 5V non-inverting buffer chip. To protect the main control board from induced voltages on the control bus, transient-voltage-suppression diodes are provided for each input and output pin on the control bus. The safety disconnect relay, as well as the injector gate drivers and indicator LEDs, are connected to the microcontroller via open-collector Darlington transistors, provided in a ULN2003N relay driver integrated circuit (IC). 5V power is received via a 10-pin ribbon cable, while 50V and 15V power for the injector is received via an 8-pin locking connector on the high-power end of the board.

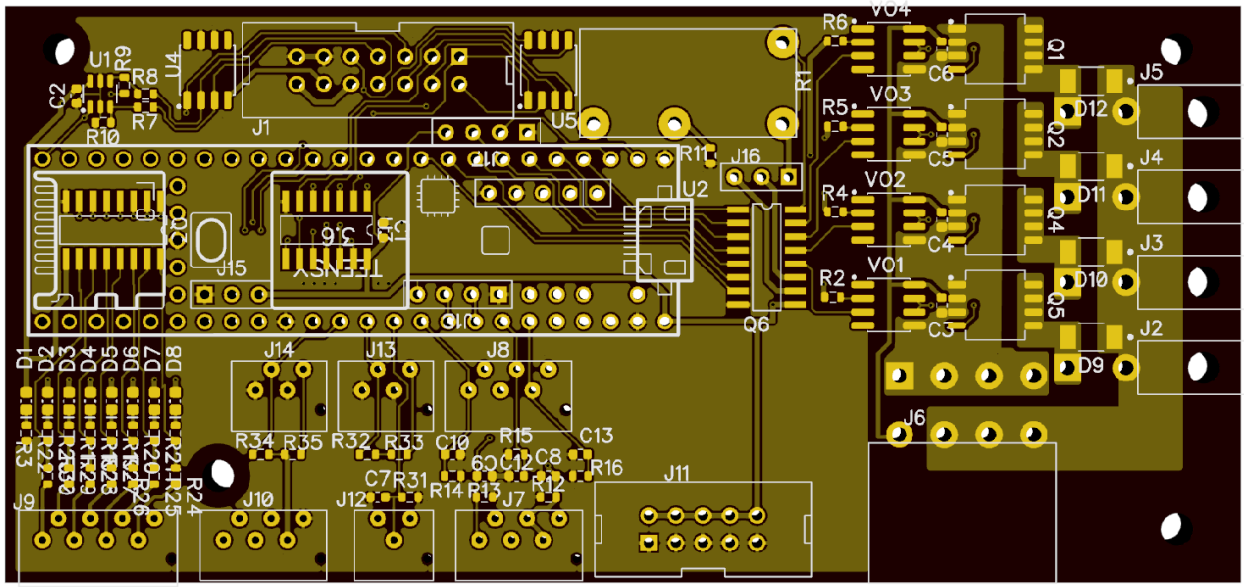

Figure 14 Main controller PCB layout

4 Mechanical Development

4.1 Considerations

4.1.1 Safety and operability

There exist several hazards with this gun. The primary mechanical hazard is the same mechanical hazard inherent to all guns: obstructing the muzzle will result in personal injury and destruction of property, as intended. While the combined weight and length of HSCG19 made shooting oneself difficult, the new design is sufficiently lightweight that this risk must be considered. The risk to bystanders must also be considered. Engineering controls to reduce these risks are difficult to conceive of, given the device in whole being developed as a system for causing harm at range. Administrative controls, though less effective [13], are required. The four ACTS of firearms safety, provided by the Royal Canadian Mounted Police [14] are adjusted and provided:

- Assume the gun is loaded at all times.
- Control the direction of the muzzle at all times, i.e., point the gun in the safest available direction.
- Trigger finger must be kept away from trigger and out of the trigger guard unless firing.
- See that the gun is unloaded before handling.

A further, though far less serious, risk is incurred due to the pinch points produced within the receiver by the injector assembly. The operator's hair or clothing may become entangled in the system during operation. The limited stroke of the injector poses little hazard but may still cause harm. The injector plunger is therefore fully enclosed except where necessary

An unexpected hazard was found during testing. The operation of the injector mechanism is quite loud, and being positioned immediately next to the operator's head, may pose a hazard to the operator's hearing. Users of the gun are instructed to wear hearing protection. This was in stark contrast to the effectively silent HSCG19.

An electrical hazard exists due to the necessary presence of high voltage electricity in the system. 50V DC can cause harm. The gun is therefore designed to prevent operator exposure to high voltages, with the sides of the busbar not being reachable from the underside of the grip region.

4.1.2 Appearance

Prior to the adoption of the project by Hacksmith, the mechanical design was focused on a lightweight package with a hemi-octagonal upper rail supporting the accelerator and an emphasis on compactness. The adoption of the project at Hackmsith brought with it a strong drive to have the design directly inspired by a popular culture icon. The MA5D assault rifle from *Halo*, shown in Figure 15, was chosen for the anticipated release of the newest installment in the *Halo* franchise, which was postponed to the following year one week after the design decision was made. A full-scale replica of the MA5D, shown in Figure 16, was 3D-printed for scale reference. It was soon found to be spectacularly large, but rather well proportioned for use by a normal person. This replica was used as a reference for all user-facing design.

Figure 15 Halo MA5D assault rifle. Copyright Bungie, Inc.

Figure 16 Halo MA5D Assault Rifle model with 6'2"engineering student for scale

Several recognizable components were retained between the designs, including the plates on the rear of the gun to provide internal mounting space for the control and supply electronics and the generally boxy shape. The new design was intended to be smaller than the previous design, however, compared to the HSCG19, the HSCG2020 design is longer and taller, as shown in Figure 17 and Figure 18. Due to the change in design methodology, it is lighter than HSCG19, which ultimately serves the goal of allowing the gun to be more easily handled.

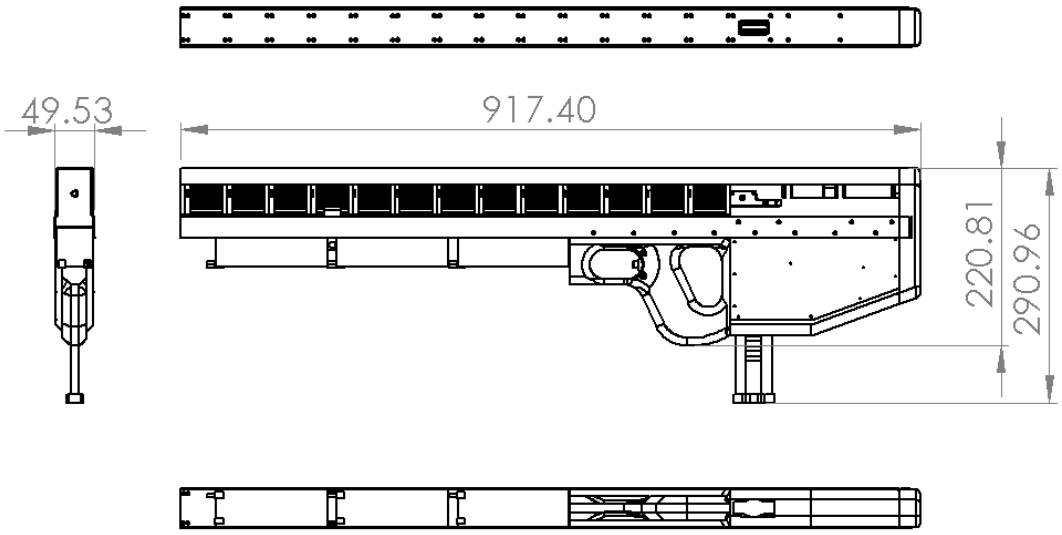

Figure 17 HSCG2020 full assembly with bounding box dimensions, indicated with and without magazine installed. Optics removed.

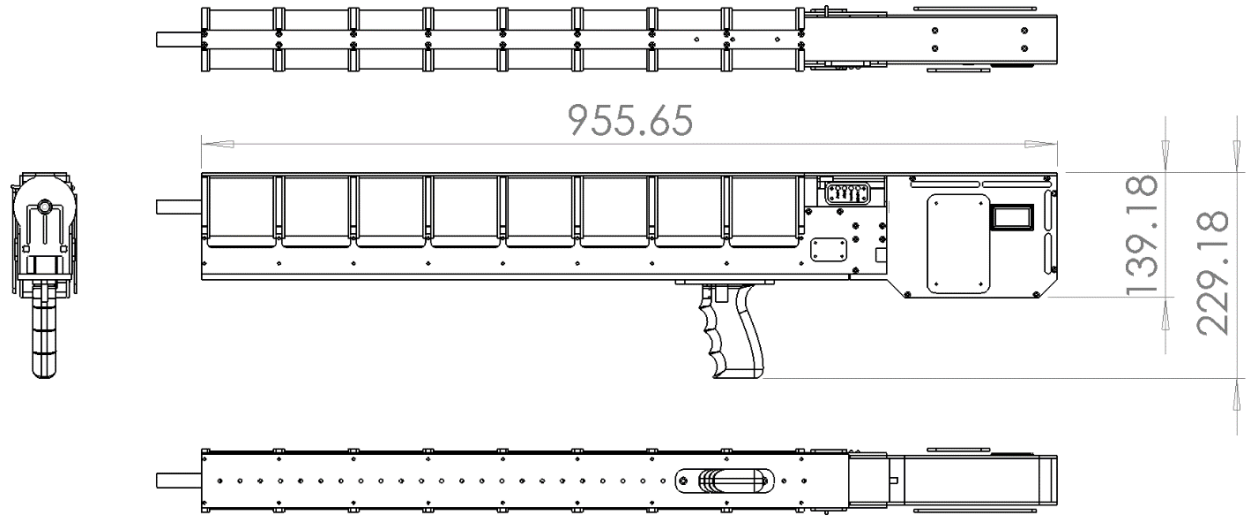

Figure 18 HSCG19 with bounding box dimensions, indicated with and without pistol grip isntalled. Optics removed.

The final design of the gun is reasonably sleek and appears compact (Figure 19). Optics or sights may eventually be included along the upper rail. The installation of the Halo cosmetic components will dramatically alter the final appearance, but the unshrouded functional assembly has its own futuristic appearance, nonetheless.

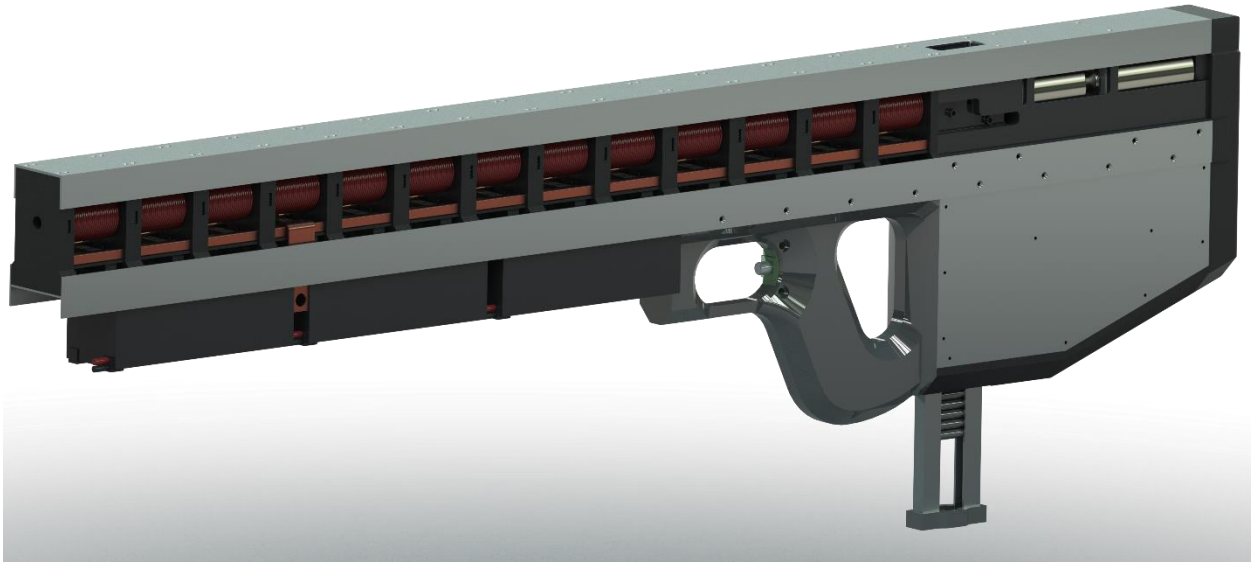

Figure 19 Final complete gun rendering

4.1.3 Tools and materials

The accessibility, convenience, and consistency of computer-numerical-control (CNC) plasma cut sheet steel in the Hacksmith Entertainment workshop made for an attractive method of construction, but it was not ultimately selected. The use of a single bent piece of steel was strongly considered but abandoned in favour of CNC-machined standard aluminum channels for weight, cost, and convenience. The availability of fusion-deposition-manufacturing (FDM) 3D-printed parts in the Hacksmith lab made them tremendously valuable to the design. The use of heat-set threaded inserts allowed for the convenient installation of threaded holes in the 3D-printed parts.

For the barrel, a thin-walled tube with an inner diameter of 0.25in, or 6.35mm, was required. This diameter provides clearance around the 6mm projectile, while also broadening the selection of available materials versus metric dimensioned material. Phenolic-infused paper, sold under the trade name “Garolite XX”, was found to be the thinnest-walled material sold in a 0.25in tube, with a 1/32in wall. The reduction in wall thickness permits more windings of copper in the solenoid for the same resistance, facilitating higher performance.

4.2 Design

The mechanical assembly of the gun is composed of several key subassemblies which are mated and retained with screws. The accelerator assembly is composed of all the stages, busbars, and associated wiring. The grip contains the user controls. The receiver contains the loading mechanism. The stock contains the controls electronics, the magazine well, and the buttplate. A cosmetic shell will be added at some future point, tying together the Halo visual theme.

4.2.1 Accelerator assembly

The accelerator assembly consists of the busbars, stage printed circuit boards, coils, feedback electronics, and the barrel. Each stage is constructed as a tightly bound assembly that can be individually tested and repaired when not installed in the gun. All 13 of these assemblies are attached to the power delivery busbars, holding them essentially coaxial, before being installed in the aluminum channels as a set, guaranteeing collinearity.

Each stage assembly is friction-fit and soldered together, requiring no fasteners. They are then secured to the aluminum channels with M2x0.4 flathead machine screws set into flanged heat-set threaded inserts in the top and bottom faces of the separator plates.

The connection, internal to the assembly, of the power switch board to the stage controller is made via a 4-pin 1.27mm-pitch right-angle header, which connects between the two boards when the power switch board is slid onto the leads of the coil itself to be secured. The tight fit between the power switch PCB and the stage separator, Figure 20, secures the busbar to which the PCB is bolted to the rest of the gun.

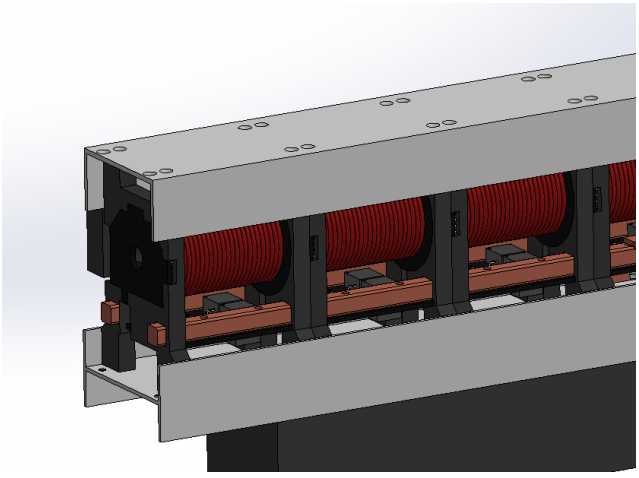

Figure 20 Portion of barrel subassembly showing coils, busbars, power switch PCB, and controller PCB..

4.2.2 Receiver assembly

The receiver exists to strip rounds from the magazine and insert them into the first stage of the accelerator. In a usual firearm, this task is accomplished using either some of the energy released from the propellant in the case of automatic loading firearms, or manually by the operator. Since there is no spare energy in the form of compressed gas or significant recoil, any design for a self loading coilgun will have to make use of additional power. Even though the electrical design goal is to make use of all available power from the batteries in the accelerator, the full 77,000W of power is available while the accelerator is inactive in between shots.

Due to time constraints, the simplest option that came to mind was adopted for inserting rounds into the barrel. This device became known as the injector assembly. The injector assembly, or just injector, makes use of a push solenoid to move the projectile from the magazine into the barrel. Initially, the use of a coil spring to reset the mechanism was considered, but this was found in testing to be too slow to successfully fire at 10Hz. A second solenoid was added to pull the solenoid plunger backwards between shots, permitting operation at upwards of 10Hz.

Operation above 12Hz is currently made difficult due to the inductance of the injector solenoids failing to produce changes in force due to changing applied voltage. Improvement of the design for a higher rate of fire was not considered a reasonable objective, having already reached 10Hz.

The two solenoids are held coaxial to one another and share a single steel plunger that impinges upon the topmost round in the magazine, as shown in Figure 21. The magazine itself is arranged such that the uppermost inner edge of the feed lip is tangent to the inside of the barrel, permitting the forward stroke of the injector plunger to advance the projectile into the barrel smoothly. The friction on the projectile due to the force of the magazine springs tends to prevent the projectile from being propelled down the barrel by the injector, though this behaviour is not necessary to the function of the gun.

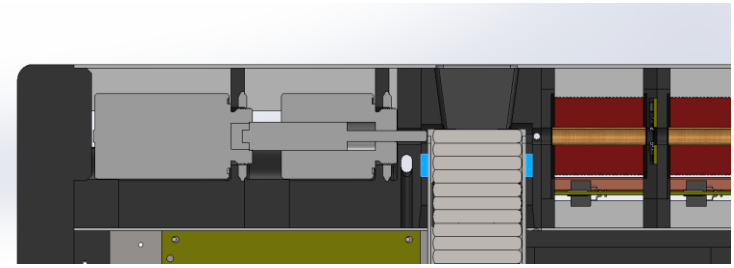

Figure 21 Injector assembly. Bore extends rightward. Magazine upper ring in blue.

To ensure smooth operation of the injector, a set of infrared object detectors are installed in the receiver assembly to detect the presence of a projectile at the top of the magazine, and the passage of a projectile out of the front of the receiver when firing. These signals are used to determine when the magazine has successfully advanced a round – and subsequently, whether the magazine is empty, and whether the most recent attempt to fire the gun was successful.

To protect the infrared detectors from stray light that could interfere with it, the sensors are embedded within the 3D-printed receiver frame and covered with opaque panels that are secured with M2 machine screws. The receiver frame is held to the main chassis rails via a set of heat-set threaded inserts on the top face and the side faces to guarantee coaxiality with the barrel.

4.2.3 Magazine

A design for a simple box-style magazine was required. The design was adapted from *Leandro*'s design [15] and modified to suit the available production tools and timelines, as well as the size of projectile in use. The adapted design (Figure 22) consists of two 0.25in inner-width extruded aluminum channels milled to length and with an open slot cut down their web. The open slot was peened into a round opening using a 0.25in tungsten carbide mandrel. This round opening formed the feed lip of the magazine, permitting rounds to be retained by friction against the inner surface of the lip, but readily forced out from behind by a small force. Rubber bands were chosen for the magazine spring, supplying tension against a 3D-printed follower that impinges upon the last round in the magazine, while not tripping the infrared detector at the top of the magazine when there are no projectiles remaining.

Figure 22 Prototype 13-round magazine

To ensure the repeated installation height of the magazine, a plastic ring was 3D-printed and secured with cyanoacrylate glue to the periphery of the aluminum extrusions, tangential to the lower edge of the feed lip openings. This ensured that the topmost projectile would always be aligned with the barrel, and so ready to be driven forwards by the action of the injector. This ring also serves as the upper connection point for the elastics.

4.2.4 Stock assembly

The key mechanical purpose of the stock is to contain the electronics that are not part of the accelerator. The secondary purpose is to make the gun comfortable to wield.

During the PCB layout stage of the design, the plan revolved around coplanar boards arranged next to one another for the power supply and distribution board and the main controller board. With the Halo redesign, the two boards wound up having to share a footprint, as viewed from the side of the gun, requiring some careful design to get the two assemblies to comfortably coincide, and dramatically increasing the width of the stock of the gun. The width of the lower accelerator rail already accommodated this increased width without significant aesthetic sacrifice.

To serve the secondary function, a thermoplastic polyurethane (TPU) buttplate was 3D-printed to cover the rear of the stock assembly. This plate serves to increase friction with the user's shoulder and absorb recoil impulse, increasing user comfort. The use of a low 3D-printing infill resulted in a very lightweight part that could deform under pressure, creating a reasonably comfortable butt for the user. The buttplate is secured to the upper aluminum channel and the stock side plates with M3 screws threaded through the mating component and into heat-set inserts pressed into the buttplate.

4.2.5 Other components

The aluminum H-channel used for the lower chassis rail was sized to fit the edge of the hardcase batteries in use. A loose friction fit was achieved. Use of pressure-sensitive tape or zip-ties will fully secure the battery both in the vertical and bore directions. The upper aluminum channel features a cut-out overtop of the magazine well to permit insertion of a sharp stick with which to clear malfunctions of the feeding system.

The through-hole grip on the gun is modelled off the Halo MA5D. It serves as a housing for the safety switch and the trigger switch, both of which are wired directly to the main controller board

in the stock of the gun. The side panels of the stock are fashioned from waterjet cut 16-gauge aluminum sheet and are secured to the underside of the H-channel with M3 rivet-nuts.

5 Control and Software Design

Optimal performance from a coilgun is achieved by optimizing the timing for the activation of the coil switches. Ideally, the feedback system could permit for automatic determination of the timing, but the additional complexity of performing this task was deemed unnecessary.

To simplify development, the microcontroller was programmed in C++ in the Arduino programming environment. The program implements a finite state machine (FSM) to manage the state of the gun and ensure that the devices operates as safely and quickly as possible. To enable real-time feedback to a connected PC and the setting of the indicator lights on the machine, a set of simple tasks are run concurrently to the FSM operation. These concurrent tasks are paused during the timing critical firing operations.

The state overview of the FSM is shown in Table 1.

Table 1 Finite state machine states

State	**Operations**	**Transitions**
Startup	Disconnect arming switch Set injector to reverse travel	Awaiting Magazine, 100ms delay
Awaiting Magazine	Disconnect arming switch Set injector to reverse idle Extinguish “Armed” indicator	Magazine Present, upon magazine detection signal
Magazine Present	Disconnect arming switch Set injector to reverse idle Extinguish “Armed” indicator	Awaiting magazine, upon magazine detection signal lost Ready To Fire, upon user engaging arming switch
Ready To Fire	Light “Armed” indicator Connect arming switch	Magazine Present, upon user disengaging arming switch Awaiting Magazine, upon absence of magazine detection signal. Firing Start, upon user engaging trigger.
Firing Start	Pulse injector forward for 15ms, then reverse Reverse injector after 15ms, or chamber sensor tripped.	Firing, upon chamber sensor tripped. Sear Holdoff, 30ms delay

Firing	Record firing has occurred. Perform staged firing sequence.	Sear Holdoff upon completion
Sear Holdoff	Set injector to reverse idle. Extinguish firing indicator. Disable all stages.	Ready To Fire upon, if in automatic: - Adjustable time delay Else: - Release trigger
Fire Error	Disable everything Blink error indicator.	NONE, this is not a recoverable state.

5.1 Tuning process

As with HSCG19, there are a few readily determined rules for setting performance expectations when tuning the gun:

1. With optimal timing, the kinetic energy imparted to the projectile by each stage will be equal, since the force applied to the projectile is a function not of time but of distance, leaving the same work being done by each stage.
2. Because of 1., the velocity of the projectile should increase with the square root of the active coil count.
3. If the velocity of the projectile compared to the stage count matches the prescribed curve, then the optimal performance has likely been achieved.

Since the design calls for fully identical coils at each stage, the imparted kinetic energy per stage should be almost perfectly equal.

Tuning is to be accomplished by iteratively adjusting the timing of the forwardmost active stage, activating the next stage whenever a performance peak is found. This method, applied to HSCG19, found optimal performance after fewer than 200 shots, with each stage's optimal timing usually be found after under 20 shots. Since HSCG20 uses identical stages, the issues with reaching ideal performance scaling at later stages that were encountered in HSCG19 will not be present, having been due to asymmetric stages and differences in coil current causing premature MOSFET failure, preventing full stage energy from being delivered reliably. Performance was measured with an optical ballistic chronograph placed directly in front of the muzzle of the gun to minimize error and minimize the risk of striking the chronograph with a projectile.

With additional programming effort, the more robust feedback elements of HSCG20 should permit the measurement of the projectile velocity to take place without external tools. This, coupled with the fully computerized nature of the gun, could permit for fully autonomous tuning of the stage timings with no user intervention required except to reload the gun. While this is an interesting thought experiment, it is not within the purview of this project, and would also be extremely dangerous.

6 Conclusion

6.1 Project Status

At the end of August 2020, the design for the coilgun was complete and construction was underway. A series of incidents involving errors in manufacture and computer failures resulted in delays that pushed the completion date of the project beyond the end of the work term. The project's future is uncertain, although an ongoing effort is being made to complete it eventually. Tests during the design phase have proven the magazine and injector designs to be effective. Mitigations have been developed and proven for all the errors discovered in the printed circuit boards. The first shot was fired August 21st, 2020, with a functioning injector and a single accelerator stage, though with a suboptimal coil design and none of the final mechanical components in place. Due to what are believed to have been software errors, several stage switches were destroyed in plumes of smoke and flame on September 13th without firing a single projectile. Work is ongoing, and success of some form will eventually be had.

6.2 Results

The updated coilgun design is complete and initial work is promising. Several design flaws were found during the prototyping phase, all of which were successfully mitigated. The simulation methodology for the accelerators has proved effective as a relative performance metric, although further refinement is in order as the absolute values produced appear to be incorrect.

6.3 Recommendations

Deemed not within the purview of the already complicated project, several possibilities exist for further exploration and improvement. Undoubtedly, another iteration of this coilgun design lies somewhere in the future, whether or not with Hacksmith. The key goal for a future design would be the improvement of system of efficiency.

Automated tuning of the stage timings would be an interesting challenge, and while it would provide little practical use for any individual gun, it could prove useful for rapid iteration of the design or mass production of the finished product.

There exists, as always, room for improvement with performance. The projected performance is acceptable, but the legal limit has not been reached, so higher speeds and energies can be achieved

without consequence, and so, by the nature of this endeavour, must be. Doing so by increasing the stage performance and efficiency rather than the power consumption and stage count, that is, gun size and weight, would be ideal.

Overcoming the thermal limitations on the design to achieve longer sustained firing windows would permit the exploration of other means of feeding, such as belts or ammunition hoppers, or more realistically larger magazines. Forced convection cooling, phase-change cooling, liquid cooling, and Peltier cooling are all potential solutions which warrant further exploration.

Increasing the efficiency of the design through more careful management of stored energy could dramatically reduce the battery requirement. Use of an H-bridge driving circuit, while not feasible at these current levels and size constraints, could potentially permit both faster current reduction and higher efficiency compared to a flyback diode and low-side single switch.

Analysis of additional features to add to the accelerator solenoids could provide significant performance and efficiency benefits. Surrounding the coil in magnetically permeable material, such as steel or iron-embedded plastic, may have a positive impact on efficiency and performance. Simulated and experimental investigation is warranted.

References

[1] Royal Canadian Mounted Police, "Frequently Asked Questions - General - Royal Canadian Mounted Police," Royal Canadian Mounted Police, 27 September 2013. [Online]. Available: http://www.rcmp-grc.gc.ca/cfp-pcaf/faq/index-eng.htm. [Accessed 9 May 2019].

[2] HobbyKing, "Turnigy Rapid 5500mAh 4S2P 140C Hardcase Lipo Battery Pack w/XT90 Connector (ROAR Approved)," HobbyKing, 2020. [Online]. Available: https://hobbyking.com/en_us/turnigy-rapid-5500mah-4s2p-140c-hardcase-lipo-battery-pack-w-xt60-connector-roar-approved.html. [Accessed January 2020].

[3] B. Hansen, "Barry's Coilgun Designs," [Online]. Available: https://www.coilgun.info/about/home.htm. [Accessed 9 May 2019].

[4] Barrett, "Model 82A1 Operator's Manual," [Online]. Available: https://barrett.net/pdf/products/Model-82A1/Manual-82A1.pdf. [Accessed July 2020].

[5] C. Holtforster, "Development of an Electromagnetic Projectile Device," 2019. [Online]. Available: https://choltfo.github.io/pub/Documents/Coilgun_2019_04_Holtforster.pdf. [Accessed 2020].

[6] International Rectifier, "IRFS4115PbF," 3 September 2011. [Online]. Available: https://www.infineon.com/dgdl/irfs4115pbf.pdf?fileId=5546d462533600a401535636e5d2218f. [Accessed 9 May 2019].

[7] NXP Semiconductors Inc., "AN11599 Using power MOSFETs in parallel," 7 July 2015. [Online]. Available: https://assets.nexperia.com/documents/application-note/AN11599.pdf. [Accessed 20 January 2020].

[8] Tyco Electronics Corporation, "Application Note: Coil Suppression Can Reduce Relay Life," [Online]. Available: http://www.te.com/commerce/DocumentDelivery/DDEController?Action=srchrtrv&DocNm=13C3264_AppNote&DocType=CS&DocLang=EN. [Accessed July 2018].

[9] Ohmite, "Res Tdh50 | Ohmite Mfg Corp," May 2020. [Online]. Available: https://www.ohmite.com/assets/docs/res_tdh50.pdf.

[10] ST Microelectronics, "100 V, 40 A Field-Effect Rectifier Diode (FERD)," March 2019. [Online]. Available: https://www.st.com/en/diodes-and-rectifiers/ferd40h100s.html. [Accessed August 2020].

[11] Silicon Labs, "Si826x, 5KV LED EMULATOR INPUT, 4.0 A ISOLATED GATE DRIVERS," March 2020. [Online]. Available: https://www.silabs.com/documents/public/data-sheets/Si826x.pdf. [Accessed July 2020].

[12] DENSEI-LAMBDA, "PAH-S48 SERIES NOTES," 1 December 1999. [Online]. Available: https://product.tdk.com/info/en/documents/instruction_manual/pah_s48_apl.pdf.

[13] National Institute for Occupational Safety and Health National Institute for Occupational Safety and Health, "HIERARCHY OF CONTROLS," 13 January 2015. [Online]. Available: https://www.cdc.gov/niosh/topics/hierarchy/default.html. [Accessed July 2020].

[14] Royal Canadian Mounted Police, Canadian Restricted Firearms Safety Course: student handbook - 4th edition, Ottawa: Technical Documentation and Graphics Section, RCMP, 2008.

[15] Leandro, "Gauss Rifle v2.0 | Hackaday.io," 2016. [Online]. Available: https://hackaday.io/project/9249-gauss-rifle-v20. [Accessed January 2020].

[16] Hobby King USA, "Basher 4000mAh 6S 65C Hardcase Pack," [Online]. Available: https://hobbyking.com/en_us/basher-4000mah-6s-65c-hardcase-pack.html. [Accessed 14 April 2019].

[17] R. Nave, "Solenoids as Magnetic Field Sources," Georgia State University Department of Physics and Astronomy, 2016. [Online]. Available: http://hyperphysics.phy-astr.gsu.edu/hbase/magnetic/solenoid.html. [Accessed 17 April 2019].

[18] U.S. Army Ardec Standardization Office, "MIL-STD-1913," October 1989. [Online]. Available: http://www.quarterbore.com/library/pdf_files/mil-std-1913.pdf. [Accessed 28 April 2019].

[19] Infineon, "IDP45E60 - Fast Switching Emitter Controlled Diode," 5 December 2013. [Online]. Available: https://www.infineon.com/dgdl/IDP45E60_rev2_4G.pdf?folderId=db3a304314dca38901151224afae0c96&fileId=db3a30432313ff5e01237a518c6e7be9.

[20] Fairchild Semiconductor, "FOD3182 3A Output Current, High Speed MOSFET Gate Driver Optocoupler," February 2011. [Online]. Available: https://www.onsemi.com/pub/Collateral/FOD3182-D.pdf.

[21] Maxim Integrated, "GLOSSARY DEFINITION FOR INDUCTIVE KICKBACK," Maxim Integrated, [Online]. Available: https://www.maximintegrated.com/en/glossary/definitions.mvp/term/Inductive%20Kickback/gpk/175. [Accessed 2019].

[22] Assmann WSW Components, "Thermal Management: CPU heatsinks V2016B," 9 September 2018. [Online]. Available: http://www.assmann-wsw.com/us/en/products/thermal-management/cpu-heatsinks/detail/1895973/. [Accessed July 2020].

Appendix A: Axisymmetric magnetostatics simulation program

```
# Coilgun stage energy calculator
# Charles Holtforster
# 2020

from femm import *
from math import *
import matplotlib.pyplot as plt
import os


mydir="./"


# Projectile sizing:
D_p = 6 # Projectile diameter
L_p = 40 # Projectile length


# System properties
V_BAT = 50 # Volts.
N_STAGES = 10 # (unitless)
I_BAT = 1500 # A
# Battery is 2/cell, 8/pack. MOSFETs are 10.3 each, 4 in parallel, busbars are negligible, cabling is
negligible, assume 1m for other.
R_SYS = (8*3 + 1 + 2.6) * 1e-3

#COPPERRESISTIVITY = 1.68e-08 # ohm*m

Rperkm = 8.28 # 14 AWG... hmm...

# Coil dimensions:
W_mm = 1.65 # Wire diameter
D_ic = 8 # Coil inner diameter
D_oc = 28 # Coil outer diameter
L_c = 40 # Coil length

# Shunt dimensions
washerF = 0 # Build the front washer?
washerR = 0 # Build the rear washer?
sleeve = 0 # Build the shunt?

T_s = 2 # Thickness of sleeve and washer
D_s = 40 # Outer diameter of sleeve

# Problem setup:
Z_proj = -20 # Offset between front face of projectile and reverse face of copper. Shunt/washers don't
count.
Z_step = 1 # Resolution of the work calculation. 1mm to 5mm is about a 1% difference; probably ain't worth
the effort.
E_force = 0.1 # If F < E_force, stop iterating.


def runSim(simName, experimentName, csv, value):
        print ("-----------------------")
        print("Start of simulation {} - {}".format(experimentName, simName))
        print ("-----------------------")

        # CONSTANTS ##############
        PGROUP = 1
        CMAT = "14 AWG"
        PMAT = "1010 Steel"
        AMAT = "Air"
```

```
        # Wire properties
        # 14AWG -> 1.65mm
        # Equivalent area for cubic packed wires = D^2
    # Experimental packing fudge factor: 1.25
        N_Coil_est = (D_oc - D_ic)/W_mm/2 * L_c/W_mm * 1.25

        R_Coil = (pi*(D_oc - D_ic)/2 * N_Coil_est)/1000 * Rperkm/1000

        I_pk = V_BAT/(R_SYS+R_Coil) # A
        I_Coil = I_pk # Assume, poorly, that we can get the coil up to full current before the force
uptick point.
        N_Coil = N_Coil_est

        print("Coil turns:\t\t{:>10.3f}".format(N_Coil))
        print("Coil resistance:\t{:>10.3f} mOhm".format(R_Coil*1000))
        print("Coil current:\t\t{:>10.3f} A".format(I_Coil))

        Z_sweep = 300#-Z_proj + L_c + L_p # The maximum distance to move the projectile, but stop if step
work goes negative or zero

        def drawRect(x1,y1, x2,y2):
                mi_addnode(x1,y1)
                mi_addnode(x2,y1)
                mi_addnode(x2,y2)
                mi_addnode(x1,y2)

                mi_addsegment(x1,y1, x2,y1)
                mi_addsegment(x2,y1, x2,y2)
                mi_addsegment(x2,y2, x1,y2)
                mi_addsegment(x1,y2, x1,y1)


        # BUILD THE SIMULATION ###############

        # Make a new magnetostatics document
        newdocument(0)

        # Set up the problem and save our new scratch fille as something:
        mi_probdef(0,"millimeters","axi",1E-8)
        mi_saveas(mydir+"TEMP.fem")

        mi_getmaterial(CMAT)
        mi_getmaterial(PMAT)
        mi_getmaterial(AMAT)

        # Setup coil circuit
        # "COIL", 100A, (0 -> parallel, 1 ->series)
        mi_addcircprop("COIL", I_Coil, 1)

        ## Build the projectile, and assign it to PGROUP
        mi_addnode(D_p/2, Z_proj)
        mi_addnode(D_p/2, Z_proj-L_p)
        mi_addnode(0, Z_proj-L_p)
        mi_addnode(0, Z_proj)

        mi_addsegment(D_p/2, Z_proj,      0, Z_proj)
        mi_addsegment(0, Z_proj,                  0, Z_proj-L_p)
        mi_addsegment(0, Z_proj-L_p,      D_p/2, Z_proj-L_p)
        mi_addsegment(D_p/2, Z_proj-L_p, D_p/2, Z_proj)

        mi_addblocklabel(D_p/4, Z_proj-L_p/2)
        mi_selectlabel(D_p/4, Z_proj-L_p/2)
        mi_setblockprop(PMAT,1,0,"",0,0,0)

        # Since everything in existence is G0, we can select everything to turn it into projectile
        mi_selectgroup(0)
        mi_setgroup(PGROUP)
```

```
        ## Build the coil and maybe a shroud
        drawRect(D_ic/2, 0, D_oc/2, L_c)

        mi_addblocklabel((D_ic+D_oc)/4, L_c/2)
        mi_selectlabel((D_ic+D_oc)/4, L_c/2)
        mi_setblockprop(CMAT,1,0,"COIL",1,0,N_Coil)


        if (washerR > 0) :
                drawRect(D_ic/2, 0, D_s/2, -T_s)

                mi_addblocklabel((D_ic+D_s)/4, -T_s/2)
                mi_selectlabel((D_ic+D_s)/4, -T_s/2)
                mi_setblockprop(PMAT,1,0,"",1,0,0)

        if (washerF > 0) :
                drawRect(D_ic/2, L_c, D_s/2, L_c+T_s)

                mi_clearselected()
                mi_addblocklabel((D_ic+D_s)/4, L_c+T_s/2)
                mi_selectlabel((D_ic+D_s)/4, L_c+T_s/2)
                mi_setblockprop(PMAT,1,0,"",1,0,0)

        if (sleeve > 0) :
                drawRect(D_s/2, -T_s, D_s/2+T_s, L_c+T_s)

                mi_clearselected()

                mi_addblocklabel((D_s + T_s)/2, L_c/2)
                mi_selectlabel((D_s + T_s)/2, L_c/2)
                mi_setblockprop(PMAT,1,0,"",1,0,0)

                mi_clearselected()

                if (D_s > D_oc and (washerR and washerF)) :
                        # The airgap needs a tag, too!
                        mi_addblocklabel((D_s + D_oc)/4, L_c/2)
                        mi_selectlabel((D_s + D_oc)/4, L_c/2)
                        mi_setblockprop(AMAT,1,0,"",0,0,0)

        ## TODO: Shield/shunt/shroud


        # Create boundary (bc = 0 for Dirichlet, 1 for Neumann)
        # n,R,x,y,bc
        mi_makeABC(7,200,0,0,0)

        # Make the air... air.
        mi_clearselected()
        mi_addblocklabel(50, -10)
        mi_selectlabel(50, -10)
        mi_setblockprop(AMAT,1,0,"",0,0,0)


        # Analyze energy!
        forceMeasured = 1
        distZ = 0
        workSum = 0


        plot_z = []
        plot_f = []
        plot_H = []

        # Proceed until we've either reached the crossover point or exceeded the simulation sweep
distance.
        while (forceMeasured > 0 and distZ < Z_sweep):
```

```
                try :
                        mi_analyze()
                        mi_loadsolution()
                except:
                        input()
                mo_hidedensityplot()
                mo_hidecontourplot()


                #mo_showdensityplot(1,0,5,1E-5,"bmag")
                mo_groupselectblock(1)

                forceMeasured=mo_blockintegral(19)

                mi_selectgroup(1)
                mi_movetranslate(0,Z_step)
                distZ = distZ + Z_step
                if (forceMeasured > 0) :
                        # Convert from mm to m, then multiply by Newtons to get J
                        workSum = workSum + (Z_step/1000)*forceMeasured

                        plot_z += [distZ]
                        plot_f += [forceMeasured]
                        plot_H += [mo_getcircuitproperties("COIL")[2] /
mo_getcircuitproperties("COIL")[0]]
                #print(forceMeasured)
        #mi_close()

        print ("Stage properties")
        print ("-----------------------")


        print("Energy:\t\t\t{:>10.3f} J".format(workSum))

        # Get projectile velocity and print it
        vo = mo_blockintegral(10) # Volume, m^3
        print("Volume:\t\t\t{:>10.3f} cc".format(vo*1000000))
        rho = 8000 # kg/m^3
        print("Mass:\t\t\t{:>10.3f} g".format(vo*rho*1000))
        V = sqrt(workSum*2/(vo*rho))
        print("Velocity:\t\t{:>10.3f} m/s".format(V))

        L_wire = (pi*(D_oc - D_ic)/2 * N_Coil_est)/1000
        print("Wire length:\t\t{:>10.3f} m".format(L_wire))

        print ("-----------------------")
        print ("")
        print ("Speculative properties for N={} (velocity scale factor = {:0.3f})".format(N_STAGES,
sqrt(N_STAGES)))
        print ("-----------------------")

        print ("Muzzle energy:\t\t{:>10.3f} J".format(N_STAGES*workSum))
        print ("Muzzle velocity:\t{:>10.3f} m/s".format(sqrt(N_STAGES)*V))

        # Calculate barrel time for 10 stages
        T = 0
        for i in range(N_STAGES):
                DT = 0.050 / (V* (sqrt(i+1) + sqrt(i)) /2)
                T += DT
        print("Barrel Time:\t\t{:>10.3f} s".format(T))
        print("Available energy:\t{:>10.3f} J".format(V_BAT*I_BAT*2*T))
        print("Consumed energy:\t{:>10.3f} J".format(V_BAT*I_pk*2*T))
        print("Efficiency (2xI):\t{:>10.3f} %".format(N_STAGES*workSum*100/(V_BAT*I_pk*2*T)))
        print("Utilization (2xI):\t{:>10.3f} %".format(I_pk*2/I_BAT*100))
        print ("-----------------------")
        print ("")
        print ("")
        print ("")
```

```
        plt.cla()
        plt.plot(plot_z, plot_f)
        plt.title("Force by distance {1} ({0})".format(experimentName, simName))
        plt.ylabel('F [N]')
        plt.xlabel('Z [mm]')
        plt.savefig("{0}/Force_{1}.png".format(experimentName, simName))

        plt.cla()
        plt.plot(plot_z, plot_H)
        plt.title("Inductance by distance {1} ({0})".format(experimentName, simName))
        plt.ylabel('L [H]')
        plt.xlabel('Z [mm]')
        plt.savefig("{0}/Inductance_{1}.png".format(experimentName, simName))

        csv.write("{0},{1},{2},{3},{4},{5},{6},{7},{8},{9},{10}\n"
                .format(value, workSum, V, vo*rho*1000, T, I_Coil, R_Coil*1000, I_Coil*R_Coil,
I_Coil*T*I_Coil*R_Coil, I_Coil*T*V_BAT, L_wire))

        simFile = open('{0}/Raw_{1}.csv'.format(ExperimentName, simName), 'w')
        simFile.write('z mm,L H,F N\n')
        for i in range(len(plot_z)):
                simFile.write('{},{},{}\n'.format(plot_z, plot_H, plot_f))
        simFile.close()

        # Cleanup
        mi_close()
        mo_close()


ExperimentName = "d{0}-l{1}-FinalReport1".format(D_p, L_p)
os.mkdir(ExperimentName)

f = open('{}/Summary_{}.csv'.format(ExperimentName,ExperimentName), 'w')
f.write("Values,Energy(J),Velocity(m/s),Mass(g),Barrel Time(s),Coil Current (A),Coil Resistance
(mohm),Coil Voltage Drop(V),Ideal Energy Delivered (J),Ideal Energy Supplied (J),Wire length (m)\n")

testDescription = open('{}/Setup_{}.txt'.format(ExperimentName,ExperimentName), 'w')
testDescription.write('Projectile:\t{0}dia x {1} len\n'.format(D_p, L_p))
testDescription.write('Coil:\t\t{0}ID x {1} len\n'.format(D_ic,L_c))
testDescription.write('Supply:\t\t{0}V {1} mohm\n'.format(V_BAT,R_SYS*1000))
testDescription.close()

openfemm()
hidepointprops()

for SWEEPD in range(9,20) :
        #L_p = L_c*SWEEPD/100
    D_oc = D_ic + SWEEPD*W_mm
    runSim ("SIM_{1}_{0}".format(D_oc, ExperimentName), ExperimentName, f, D_oc)

closefemm() # Goodnight!
```